Uniplanar Hybrid Couplers Using Asymmetrical Coplanar Striplines

Brad Ryan Heimer, Lu Fan, *Member, IEEE,* and Kai Chang, *Fellow, IEEE*

***Abstract*—This paper presents four new uniplanar 3-dB hybrid couplers using asymmetrical coplanar strips (ACPS's) for microwave integrated circuit (MIC) and monolithic MIC (MMIC) applications. Experimental results show that the standard ($1.5\lambda_g$ circumference) uniplanar 180° hybrid-ring coupler has 3.5 ± 0.4 dB coupling, greater than 21-dB isolation, and greater than 23.4-dB return loss over a 25% bandwidth centered at 3 GHz. The 180° reverse-phase hybrid-ring coupler ($1.0\lambda_g$ circumference) provides better performance as compared to conventional microstrip hybrid couplers. This circuit has a bandwidth of more than one octave from 2 to 4 GHz with ±0.4-dB power dividing imbalance and ±4° phase imbalance. The 180° reduced-size reverse-phase hybrid-ring coupler ($0.8\lambda_g$ circumference) maintains the performance of the 180° reverse-phase hybrid coupler with the advantage of smaller size. This circuit also has a bandwidth of more than one octave from 2 to 4 GHz with ±0.3-dB power dividing imbalance and ±3.1° phase imbalance. A new 90° 3-dB branch-line hybrid coupler is also introduced. Experimental results show the insertion loss of this component to be 0.5 dB at 3 GHz, and also greater than 15.3-dB isolation and 17.1-dB return loss over a 10% bandwidth centered at 3 GHz. The circuits were designed and simulated with Sonnet electromagnetic-circuit solver software. The measured results agree well with the simulations.**

***Index Terms*— Coplanar striplines, coplanar waveguides, hybrid coupler, uniplanar circuits.**

I. Introduction

HYBRID COUPLERS are fundamental and important components extensively used in the realization of a variety of microwave circuits such as balanced mixers, data modulators, phase shifters, and feed networks in antenna arrays. Rat-race hybrids [1], reverse-phase hybrids [2], and crossover hybrids [3] are well-known examples of 180° hybrid couplers. Most previous work is based on microstrip structures because microstrip is the most mature and widely used transmission line. This is mainly a result of the convenience of microstrip due to the large amount of characterization and availability in commercial software design packages [4]. However, in recent years, uniplanar transmission lines such as coplanar waveguide (CPW), coplanar strip (CPS), and slotline have become a competitive alternative to microstrip with an increasing use in many applications. These transmission lines have advantages of small dispersion, simple realization of short-circuited ends, easy integration with lumped elements or active components, and no need for via holes. Many attractive uniplanar 90° and 180° hybrids have been proposed [5], [6] using these transmission lines. More recently, asymmetrical uniplanar transmission lines such as asymmetrical CPW (ACPW) [7] and asymmetrical CPS (ACPS) [8] have been used as alternatives to symmetrical ones in the design of MIC's because of the additional flexibility offered by the asymmetric configuration. The applications of ACPW and ACPS to mixers [9], attenuators [10], and power dividers [11] have been reported. To further extend the asymmetric uniplanar techniques to MIC and MMIC applications, more uniplanar components are required.

The CPW transmission line has its advantages, but when used in conjunction with hybrid rings, CPW presents the problem of having to plate the inner circular conducting ground plane, as well as bond to it at the T-junctions. This incorporates extra time and cost into the fabrication process. Several different ACPS hybrid couplers are proposed to eliminate this process, utilize the advantages of uniplanar CPW, and meet desired specifications for MIC and MMIC applications. This paper presents three new uniplanar 180° hybrid-ring couplers, and one new uniplanar 90° branch-line coupler using ACPS. These couplers have characteristics similar to those of microstrip circuits with the advantages of a uniplanar structure and better performance. The circuit simulations for the ACPS lines and hybrid couplers are performed using Sonnet Software,[1] and it will be shown that the measured results agree well with the circuit simulations.

II. Asymmetric Coplanar Stripline

The ACPS configuration consists of a ground plane on one side of the transmission line, a spacing of width (S), and a conductive strip of variable width (W_{ACPS}), as can be seen in Fig. 1. Other parameters include the height of the substrate (h), the thickness of the metal (t), and the dielectric constant (ε_r). Sonnet Software's *em* was used to characterize the ACPS transmission line. The experimental circuit in Fig. 1 was designed and fabricated on an $h = 0.635$-mm-thick RT/Duroid 6010 ($\varepsilon_r = 10.8$, $t = 18$ μm) substrate at a center frequency of 3 GHz.

Manuscript received March 24, 1997; revised August 15, 1997. This work was supported in part by Texas Instruments Incorporated, and by the U.S. Army Research Office.

B. R. Heimer was with the Department of Electrical Engineering, Texas A&M University, College Station, TX 77843-3128 USA. He is now with Raytheon TI Systems, Dallas, TX 75243 USA.

L. Fan and K. Chang are with the Department of Electrical Engineering, Texas A&M University, College Station, TX 77843-3128 USA (e-mail: chang@eesun1.tamu.edu).

Publisher Item Identifier S 0018-9480(97)08320-8.

[1]Sonnet Software is a registered trademark of Sonnet Software, Inc., Liverpool, NY.

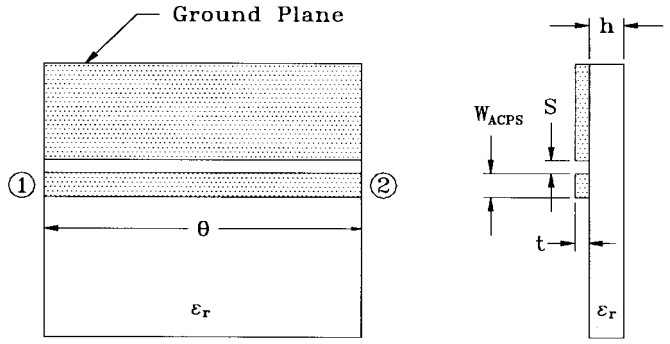

Fig. 1. ACPS configuration.

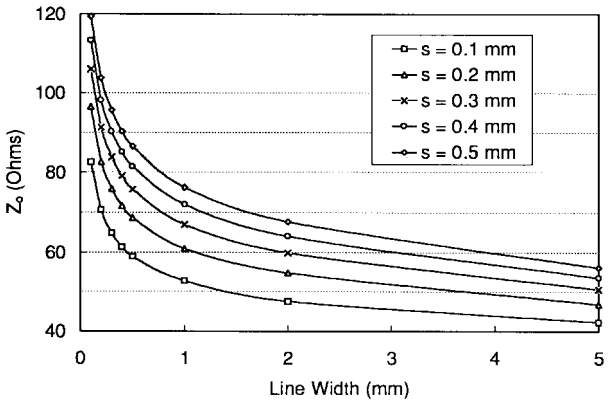

(a)

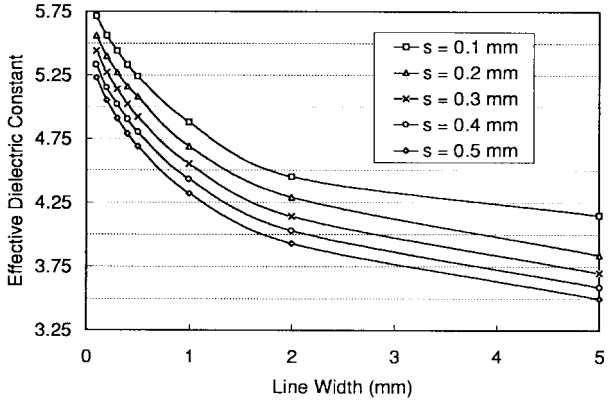

(b)

Fig. 2. Sonnet analysis of ACPS characteristics at 3 GHz. (a) Z_0 versus linewidth. (b) $\varepsilon_{\rm eff}$ versus linewidth.

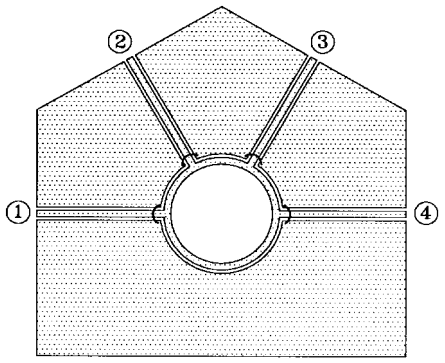

(a)

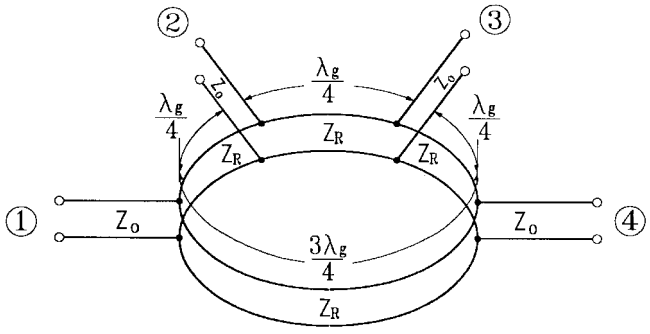

(b)

Fig. 3. ACPS 180° hybrid-ring coupler. (a) Circuit configuration. (b) Equivalent transmission-line model.

Two different graphs were generated using Sonnet to show the characteristics of the ACPS transmission line. Fig. 2(a), which shows Z_0 as a function of $W_{\rm ACPS}$, has five different traces for different spacing (S) between the transmission line and the ground plane. As can be seen, the characteristic impedance of the ACPS line ranges from 40 to 120 Ω. Higher impedance values may be obtained by making the space larger and the linewidth smaller. To achieve an impedance value lower than 40 Ω, the width to spacing ratio has to be made very large. This is impractical in most situations and, therefore, limits the low impedance values to about 35–40 Ω. Fig. 2(a) also shows that Z_0 increases as the spacing between the transmission line and ground plane increases, and that Z_0 decreases as the width of the transmission line increases. Fig. 2(b) illustrates how the effective dielectric constant $(\varepsilon_{\rm eff})$ varies over linewidth for different spacing (S) between the transmission line and the ground plane. Each trace shows a different spacing, ranging from 0.1 to 0.5 mm in increments of 0.1 mm.

Fig. 2 contributes to an understanding of the performance and limitations of using ACPS transmission lines on this particular substrate. ACPS has a characteristic impedance range of approximately 35–185 Ω, and an effective dielectric constant range of approximately 3.25–5.75 for the $\varepsilon_r = 10.8$ substrate. These graphs, along with other Sonnet simulations, will serve as the building blocks required to carry out more detailed designs of complex circuit structures.

III. Uniplanar Rat-Race Hybrid-Ring Coupler

As mentioned above, to fully utilize the advantages of asymmetric uniplanar structures, additional ACPS components need to be developed. This section describes an ACPS hybrid-ring coupler. Fig. 3(a) shows the physical configuration of the $1.5\lambda_{g,\rm ACPS}$ circumference uniplanar hybrid-ring coupler that is realized on one side of the substrate using CPW and ACPS transmission lines. The circuit consists of four CPW to ACPS T-junctions and a circular ACPS ring that is divided into three $\lambda_{g,\rm ACPS}/4$ sections and one $3\lambda_{g,\rm ACPS}/4$ section. The characteristic impedance of the circular ACPS ring is $Z_R = \sqrt{2}Z_0$, where Z_0 is the characteristic impedance of the CPW feed lines. Based on this design, an experimental

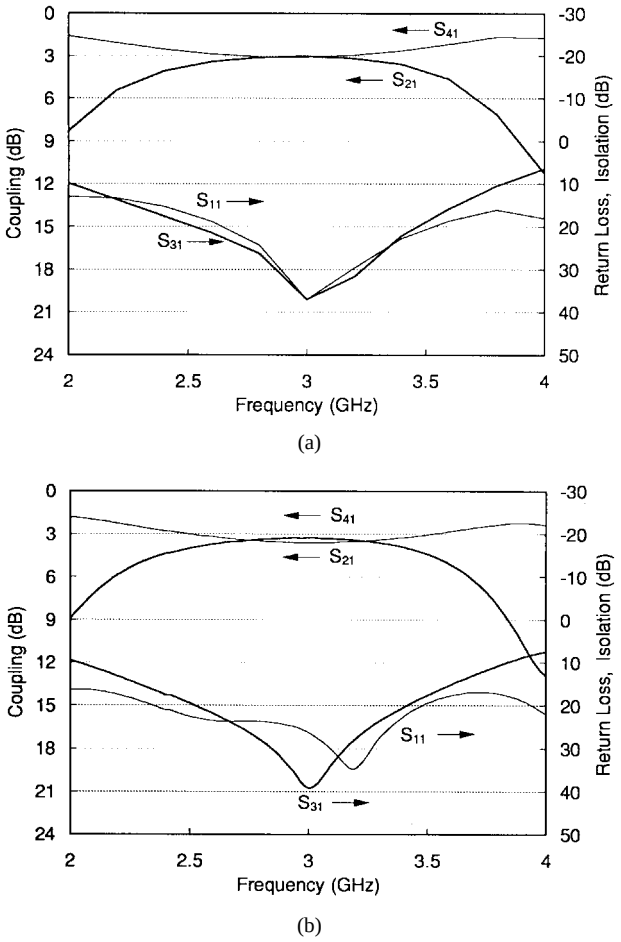

Fig. 4. Simulation and measured data for ACPS 180° hybrid-ring coupler. (a) Sonnet simulation results. (b) Measured data.

circuit was etched on an $h = 0.635$-mm-thick RT/Duroid 6010 ($\varepsilon_r = 10.8$) substrate with a characteristic impedance of $Z_0 = Z_{\rm CPW} = 50\ \Omega$ for the four CPW feed lines, and $Z_R = 71\ \Omega$ for the circular ring. Sonnet Software was used to obtain the dimensions of the ACPS transmission lines as well as to model the CPW to ACPS T-junctions at a center frequency of 3 GHz. These four CPW feeds have a gap of $G = 0.29$ mm and a center conductor width of $W_{\rm CPW} = 0.60$ mm. The 71-Ω ACPS consists of the ground plane, a space of $S = 0.27$ mm, and a linewidth of $W_{\rm ACPS} = 0.40$ mm. The quarter-wavelength sections are 10.73 mm in length. The curvature of the ACPS was not taken into consideration in the simulation because the curvature does not affect the behavior for the operation frequency. However, this is only true if the transmission line is located on the inside of the curve [12]. To eliminate the coupled slotline mode propagating on the CPW and ACPS lines, bond wires have been placed over the CPW feed lines at the T-junction of the ACPS [13]. The equivalent transmission-line model of the $1.5\lambda_{g,\rm ACPS}$ circumference hybrid ring is shown in Fig. 3(b).

The simulation of this circuit was carried out using Sonnet Software, and the results of the simulated insertion loss, return loss, and isolation are shown in Fig. 4(a). The simulated data agrees very well with the measured data, which is shown in Fig. 4(b). The measurements were made on an HP-8510 network analyzer using standard subminiature A (SMA) connectors from 2 to 4 GHz. Over a 750-MHz bandwidth centered at 3 GHz, the measured results show that the coupling ($|S_{21}|$ or $|S_{41}|$) is 3.5 $\pm$ 0.4 dB (3 dB for ideal coupling, the insertion loss is less than 0.9 dB, which includes two coaxial-to-CPW transitions and 40-mm-long input/output CPW lines), the input return loss ($|S_{11}|$) is greater than 23 dB, and the isolation ($|S_{31}|$) is greater than 21 dB. Compared to the typical microstrip hybrid-ring coupler with a typical bandwidth of 20%, the ACPS coupler has a bandwidth of 25%.

IV. 180° Reverse-Phase Hybrid-Ring Coupler

The rat-race hybrid-ring coupler is the well-known and commonly used 180° hybrid. However, the 20%–25% bandwidth of the rat-race ring coupler limits its applications to narrowband circuits, and the $1.5\lambda_g$ circumference of the ring takes up a large area of chip real estate. This directly translates to a higher cost per chip. Hybrid rings of smaller size that do not compromise performance are, therefore, a sought after component, and many have been successfully designed using a variety of techniques [14]–[19]. To extend the bandwidth with a simple design procedure and implement the uniplanar structure, this section presents a new uniplanar hybrid-ring coupler consisting of a circular ACPS ring with four CPW feeds. The design technique substitutes a 180° reverse-phase ACPS section with a length of $\lambda_{g,\rm ACPS}/4$ for the conventional $3\lambda_{g,\rm ACPS}/4$ phase delay section. Since the 180° phase shift of the ACPS reverse-phase section is not sensitive to frequency, the resulting circular ACPS hybrid coupler attains a broad-bandwidth.

A. 180° Reverse-Phase ACPS Section

Fig. 5(a) shows the circuit configuration and the E-field distribution for the ACPS reverse-phase section. This section consists of a slotline radial stub with a bond wire crossing over the ACPS transmission line. The arrows shown in Fig. 5(a) indicate the electric fields in the ACPS lines. In Fig. 1, the input signal fed to port one propagates through the line and arrives with a phase shift of θ at port two. In Fig. 5(a), the input signal fed to port one propagates through the ACPS crossover and arrives with an additional 180° phase shift at port two. Fig. 5(b) shows the measured amplitude and phase differences between the circuits in Figs. 1 and 5(a). The maximum amplitude difference is 0.5 dB from 1 to 5 GHz. The maximum phase difference is 180° $\pm$ 5° over the same frequency range. The purpose of this circuit is to replace the traditional $3\lambda_{g,\rm ACPS}/4$ section of the ring between ports one and four, shown in Fig. 3. This is accomplished by replacing a $\lambda_{g,\rm ACPS}/2$ section of transmission line by the 180° phase shifter. This transformation allows the overall circuit size to shrink, reduces the losses, and increases the bandwidth as compared with the $1.5\lambda_{g,\rm ACPS}$ circumference ACPS hybrid ring.

B. 180° Reverse-Phase Hybrid-Ring Coupler

Fig. 6(a) shows the circuit configuration of the new hybrid-ring coupler consisting of four CPW to ACPS T-junctions and

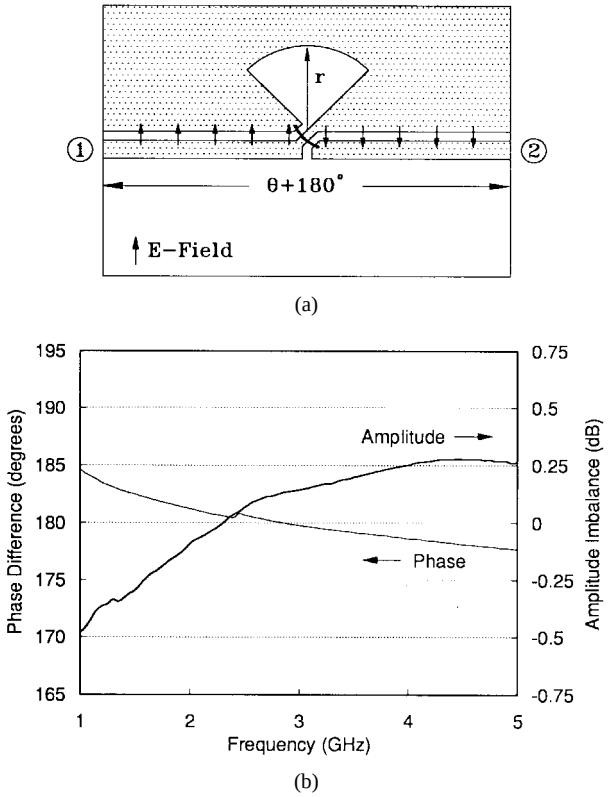

(a)

(b)

Fig. 5. ACPS 180° reverse-phase section. (a) Circuit configuration. (b) Measured amplitude and phase differences between the circuits shown in Fig. 1 and Fig. 5(a).

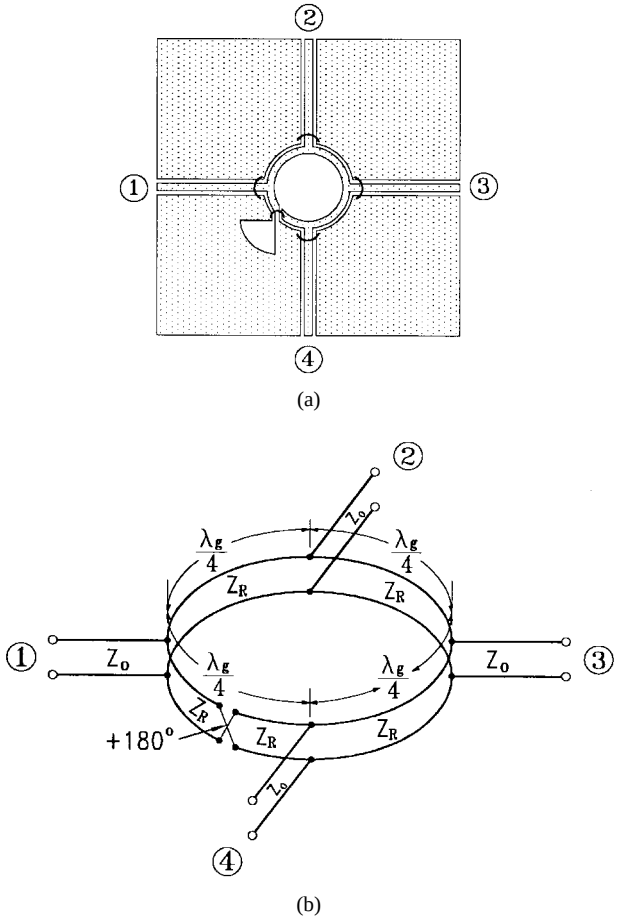

(a)

(b)

Fig. 6. ACPS 180° reverse-phase hybrid-ring coupler. (a) Circuit configuration. (b) Equivalent transmission-line model.

four ACPS arms (one of them with a 180° phase reversal). Fig. 6(b) shows the equivalent transmission-line model of the coupler. The twisted transmission line represents the phase reversal of the ACPS crossover. When the signal is fed to port one, it splits into two equal components that arrive at ports two and four in phase, but are canceled out at port three.

Similar to the case of the 180° hybrid-ring coupler in Section III, the 180° reverse-phase hybrid-ring coupler was fabricated on an $h = 0.635$-mm-thick RT/Duroid 6010 ($\varepsilon_r = 10.8$) substrate. The simulation and synthesis for the practical circuit was performed using Sonnet at a center frequency of 3 GHz. The circuit's CPW feed lines have a characteristic impedance of $Z_0 = Z_{\mathrm{CPW}} = 50\,\Omega$ (strip width $W_{\mathrm{CPW}} = 0.60$ mm, gap size $G = 0.29$ mm), and the ACPS lines have a characteristic impedance of $Z_R = \sqrt{2}Z_0 = 71\ \Omega$ (strip width $W_{\mathrm{ACPS}} = 0.40$ mm, spacing size $S = 0.27$ mm). The four ACPS arms each have a length of $\lambda_{g,\mathrm{ACPS}}/4 = 10.73$ mm. The slotline radial stub's radius is $r = 6$ mm with an included angle of 90°.

Adding air bridges at the circuit's discontinuities is important to prevent the coupled slotline mode from propagating on the CPW and ACPS lines. During testing, the circuit was connected to an HP-8510 network analyzer using standard SMA connectors. The insertion loss includes two coaxial-to-CPW transitions and 40-mm-long input/output CPW lines which were not calibrated out. The measured data of the reverse-phase hybrid coupler are shown in Fig. 7(a). Over an octave bandwidth from 2 to 4 GHz, Fig. 7(a) shows that the coupling ($|S_{21}|$ or $|S_{41}|$) is 3.95 ± 0.45 dB (3 dB for ideal coupling) and the isolation ($|S_{31}|$) is greater than 23 dB. The input return loss ($|S_{11}|$) is greater than 15 dB from 2.2 to 4 GHz, and is greater than 13.5 dB from 2 to 4 GHz. Fig. 7(b) illustrates an important feature of the coupler. The output amplitude imbalance (± 0.4 dB) and phase difference (± 4°) are excellent over a bandwidth from 2 to 4 GHz because the ACPS crossover provides an almost perfect 180° phase shift over the entire frequency range. This is an advantage with respect to the microstrip implementations of the 180° hybrid-ring coupler, where the $\lambda_g/2$ delay line gives a 180° phase shift only at the center frequency.

V. Reduced-Size 180° Reverse-Phase Hybrid-Ring Coupler

The 180° reverse-phase hybrid-ring coupler attains good performance with a ring circumference of $1.0\lambda_{g,\mathrm{ACPS}}$. This circuit's size may be reduced even further by using a particular design formula. The characteristic impedance of the ACPS transmission line that makes up the ring is given by the following equation [20]:

$$Z_R = Z_0\sqrt{2(1 - \cot^2\theta)}.$$

In this equation, Z_0 is the 50-Ω port impedance, and θ is the electrical length of one arm, which has a range of $45° \leq$

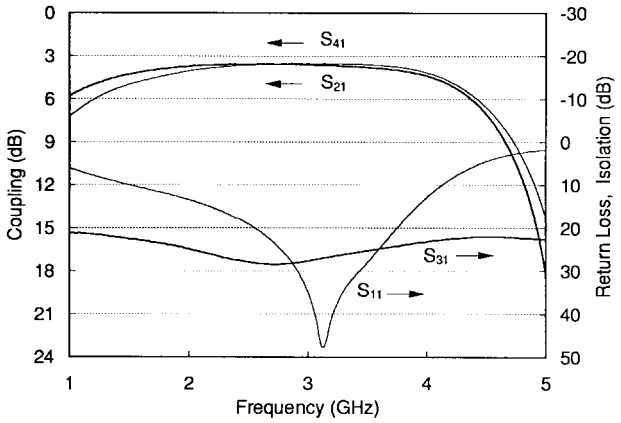

(a)

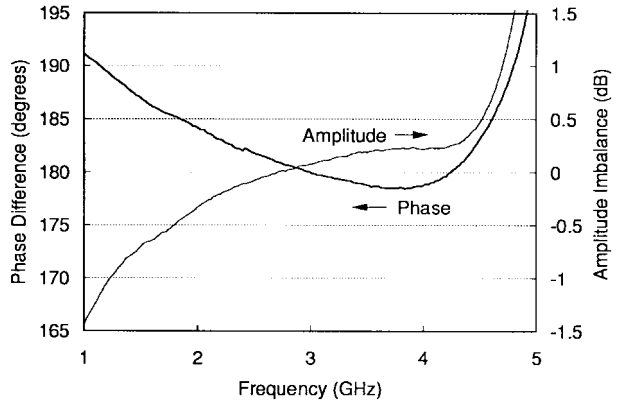

(b)

Fig. 7. Measured results for ACPS 180° reverse-phase hybrid-ring coupler. (a) Coupling, return loss, and isolation. (b) Amplitude imbalance and phase difference.

$\theta \leq 90°$. In the previous designs of the hybrid ring and reverse-phase hybrid ring, the length of the ACPS transmission-line sections have been $\lambda_{g,\mathrm{ACPS}}/4$, or $\theta = 90°$. From the design formula, substituting $\theta = 90°$ gives $Z_R = Z_0\sqrt{2}\ \Omega$. In the design of the reduced size reverse-phase hybrid ring, θ will be set equal to 72° and the characteristic impedance of the ACPS lines is solved to be $Z_R = 66.9\ \Omega$. An electrical length of 72° is the same as a line length of $\lambda_{g,\mathrm{ACPS}}/5$, so the new reduced size reverse-phase hybrid-ring coupler will have an overall circumference of $4(\lambda_{g,\mathrm{ACPS}}/5)$, or $0.8\lambda_{g,\mathrm{ACPS}}$. This is a substantial reduction in size from the $1.5\lambda_{g,\mathrm{ACPS}}$ hybrid-ring coupler and can save some costs in fabrication. The equivalent-circuit model of this new structure is shown in Fig. 8.

Fig. 9(a) shows that the reduced size reverse-phase hybrid ring's bandwidth remains equal to an octave from 2 to 4 GHz. In this bandwidth, the coupling ($|S_{21}|$ or $|S_{41}|$) is 3.5±0.4 dB (3 dB for ideal coupling, includes a 30-mm section of CPW transmission line and two coaxial to CPW connectors which were not calibrated out) and the isolation ($|S_{31}|$) is greater than 29.8 dB. The input return loss ($|S_{11}|$) is greater than 15 dB from 2.2 to 4 GHz, and is greater than 12 dB from 2 to 4 GHz. Fig. 9(b) shows that the amplitude imbalance is ± 0.3 dB and the phase difference is ± 3.1° from 2 to 4 GHz.

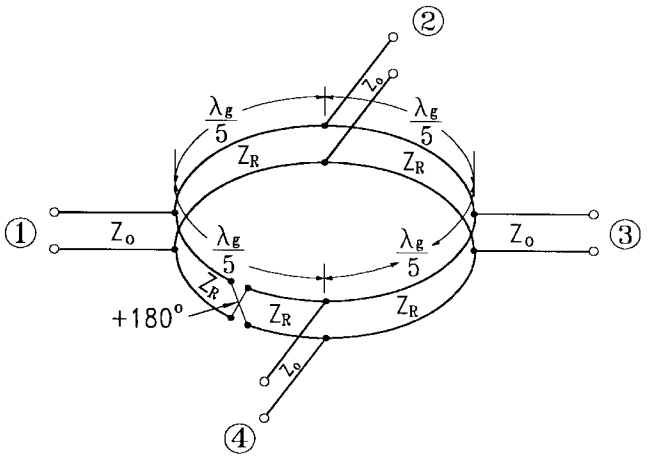

Fig. 8. Equivalent-circuit model of ACPS 180° reduced size reverse-phase hybrid-ring coupler.

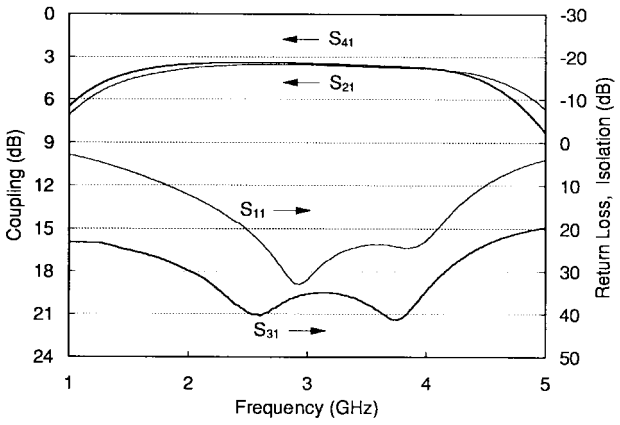

(a)

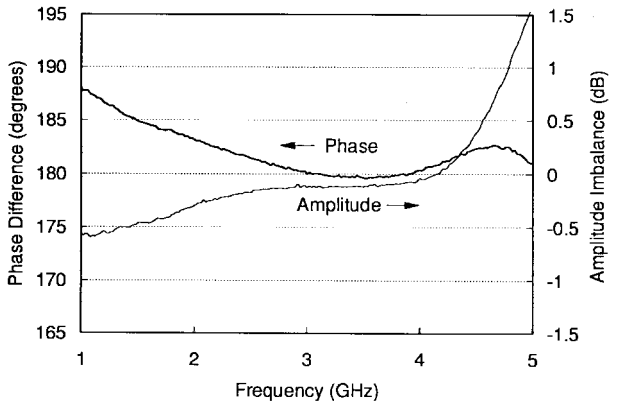

(b)

Fig. 9. Measured results for the circuit shown in Fig. 8. (a) Coupling, return loss, and isolation. (b) Amplitude imbalance and phase difference.

All measurements were made on an HP-8510 network analyzer using standard SMA connectors from 1 to 5 GHz.

VI. ACPS Branch-Line Coupler

The 90° ACPS branch-line hybrid coupler is shown in Fig. 10(a). In a standard branch-line coupler, if the port characteristic impedance is Z_0, then two of the $\lambda_g/4$ branches have a

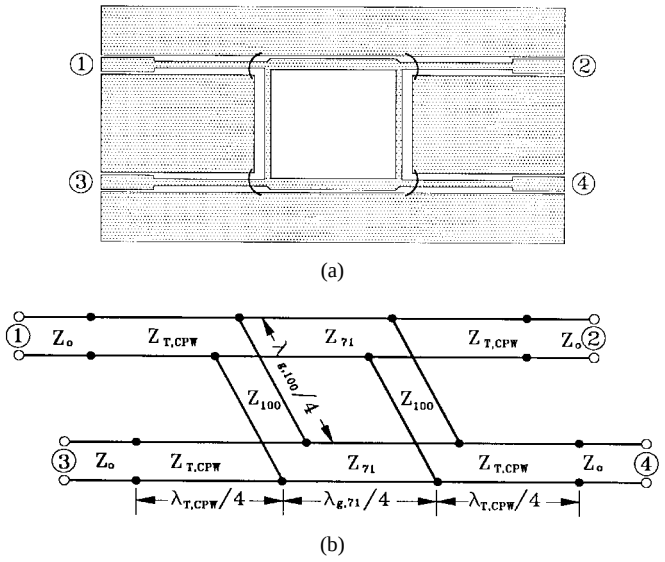

Fig. 10. ACPS 90° branch-line coupler. (a) Circuit configuration. (b) Equivalent transmission-line model.

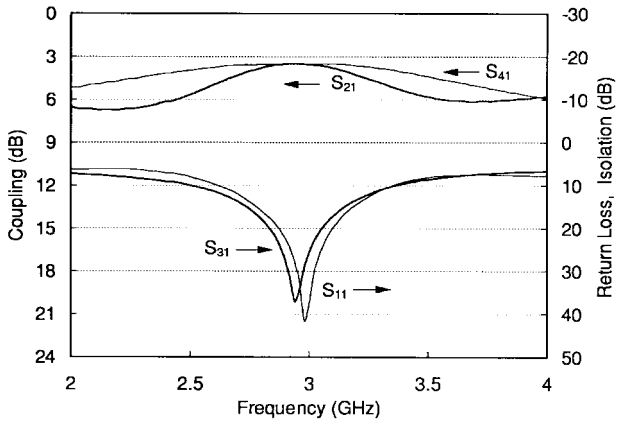

Fig. 11. Measured coupling, return loss, and isolation for ACPS 90° branch-line coupler.

characteristic impedance of Z_0 and two of the $\lambda_g/4$ branches have a characteristic impedance of $Z_0/\sqrt{2}$. If $Z_0 = 50\ \Omega$, then the two $Z_0/\sqrt{2}$ lines would each have a characteristic impedance of 35.4 Ω. Referring to Section I, this impedance value is difficult to attain using ACPS. To overcome this problem, the input and output port characteristic impedances were increased to Z_0' (100 Ω). By using a CPW quarter-wavelength transformer, the coupler port impedances ($Z'_{\rm CPW} = Z_0' = 100\ \Omega$) were matched to the CPW ($Z_{\rm CPW} = Z_0 = 50\ \Omega$), which can be connected to the standard 50-Ω test equipment. Based on the above consideration, two high-impedance branches ($Z_{100} = Z_0' = 100\ \Omega$) and two low-impedance branches ($Z_{71} = Z_0'/\sqrt{2} = 71\Omega$) were designed. The equivalent circuit for this branch-line coupler is shown in Fig. 10(b). The 71-Ω ACPS branch line ($\lambda_{g,71}/4 = 11.07$ mm) has a spacing of $S = 0.20$ mm and a linewidth of $W_{\rm ACPS} = 0.42$ mm. The 100 Ω ACPS branch line ($\lambda_{g,100}/4 = 10.96$ mm) has a spacing of $S = 0.40$ mm and a linewidth of $W_{\rm ACPS} = 0.18$ mm. For the CPW quarter-wavelength transformer section ($\lambda_{T,\rm CPW}/4 = 10.81$ mm, $Z_{T,\rm CPW} = 71\ \Omega$), a gap of $G = 0.40$ mm and a linewidth of $W_{T,\rm CPW} = 0.23$ mm are used.

The CPW to ACPS T-junctions were simulated using Sonnet, as well as the ACPS transmission lines. Bond wires were once again attached over the CPW feed lines at the T-junctions to keep the coupled slotline modes from propagating. The branch-line coupler was fabricated on an $h = 0.635$-mm-thick RT/Duroid 6010 ($\varepsilon_r = 10.8$) substrate. Fig. 11 shows that the branch-line coupler has attained a 10% bandwidth centered at 3 GHz. The coupling is 3.5 dB at 3 GHz (3 dB for ideal coupling, the insertion loss includes two CPW quarter-wavelength transformers of length 21.8 mm, two CPW input/output sections of length 10 mm, and two coaxial to CPW connectors which were not calibrated out). The input return loss is greater than 17.1 dB and the isolation is greater than 15.3 dB. The coupler has a worst-case amplitude imbalance of 0.375 dB and a worst-case phase imbalance of 1.9° over the specified bandwidth. All measurements were made on an HP-8510 network analyzer using standard SMA connectors from 2 to 4 GHz.

VII. Conclusion

ACPS is a relatively new uniplanar transmission line with many advantages. ACPS requires an electromagnetic circuit solver such as Sonnet to accurately characterize the transmission line, and can be applied to the design of hybrid couplers. The design procedure and results of these newly developed 180° hybrid couplers were described. The uniplanar hybrid couplers demonstrated a good amplitude imbalance and phase difference over a wide bandwidth. With its advantages of a compact, simple, uniplanar structure and ease of integration with solid-state devices, these uniplanar hybrid couplers will be useful in many MIC and MMIC applications.

References

[1] C. Y. Pon, "Hybrid-ring directional couplers for arbitrary power division," *IRE Trans. Microwave Theory Tech.*, vol. MTT-9, pp. 529–535, Nov. 1961.
[2] E. M. Jones, "Wide-band strip-line magic-T," *IRE Trans. Microwave Theory Tech.*, vol. MTT-8, pp. 160–168, Mar. 1960.
[3] C. H. Ho, L. Fan, and K. Chang, "Ultra wide band slotline hybrid-ring couplers," in *IEEE MTT-S Int. Microwave Symp. Dig.*, Albuquerque, NM, June 1992, pp. 1175–1178.
[4] M. Gillick, I. D. Robertson, and A. H. Aghvami, "Uniplanar techniques for monolithic microwave integrated circuits," *Electron. Commun. Eng. J.*, pp. 187–194, Aug. 1994.
[5] T. Hirota, Y. Tarusawa, H. Ogawa, and K. Owada, "Planar MMIC hybrid circuit and frequency converter," in *IEEE MTT-S Int. Microwave Symp. Dig.*, Baltimore, MD, June 1986, pp. 103–105.
[6] C. H. Ho, L. Fan, and K. Chang, "Broad-band uniplanar hybrid-ring and branch-line couplers," *IEEE Trans. Microwave Theory Tech.*, vol. 41, pp. 2116–2125, Dec. 1993.
[7] V. F. Hanna and D. Thebault, "Theoretical and experimental investigation of asymmetric coplanar waveguide," *IEEE Trans. Microwave Theory Tech.*, vol. MTT-32, pp. 1649–1651, Dec. 1984.
[8] I. Kneppo and J. Gotzman, "Basic parameters of nonsymmetrical coplanar lines," *IEEE Trans. Microwave Theory Tech.*, vol. MTT-25, p. 718, Aug. 1977.
[9] D. Jaisson, "A single-balanced mixer with a coplanar balun," *Microwave J.*, vol. 35, pp. 87–96, July 1992.
[10] D. Jaisson, "A microwave-coplanar waveguide coupler for use with an attenuator," *Microwave J.*, vol. 38, no. 9, pp. 120–130, Sept. 1995.
[11] L. Fan and K. Chang, "Uniplanar MIC power dividers using coupled CPW and asymmetrical CPS," in *IEEE MTT-S Int. Microwave Symp. Dig.*, San Francisco, CA, May 1996, pp. 781–784.

[12] D. Jaisson, "An asymmetrical coplanar waveguide for use with a coplanar Wilkinson power divider," *Microwave J.*, vol. 35, no. 7, pp. 68–76, Nov. 1995.
[13] M. Riazat, S. Bandy, and G. Zdasiuk, "Coplanar waveguides for MMIC's," *Microwave J.*, pp. 125–131, June 1987.
[14] L. Fan, C. H. Ho, S. Kanamaluru, and K. Chang, "Wide-band reduced size uniplanar magic-T, hybrid-ring, and de Ronde's CPW-slot couplers," *IEEE Trans. Microwave Theory Tech.*, vol. 43, pp. 2749–2758, Dec. 1995.
[15] B. D. Brewster, I. D. Robertson, and O. Gemikonakli, "Design and realization of a reduced-size microstrip 3-dB rat race hybrid coupler," *Microwave Opt. Technol. Lett.*, vol. 6, no. 14, pp. 789–790, Nov. 1993.
[16] T. Hirota, A. Minakawa, and M. Muraguchi, "Reduced-size branch-line and rat-race hybrids for uniplanar MMIC's," *IEEE Trans. Microwave Theory Tech.*, vol. 38, pp. 270–275, Mar. 1990.
[17] C. Nguyen, "A new compact ring hybrid and its use in a singly balanced mixer," *Microwave Opt. Technol. Lett.*, vol. 7, no. 16, pp. 732–733, Nov. 1994.
[18] D. I. Kim and Y. Naito, "Broad-band design of improved hybrid-ring 3-dB directional coupler," *IEEE Trans. Microwave Theory Tech.*, vol. MTT-30, pp. 2040–2046, Nov. 1982.
[19] D. I. Kim and G. S. Yang, "Design of a new hybrid-ring directional coupler using $\lambda/8$ or $\lambda/6$ sections," *IEEE Trans. Microwave Theory Tech.*, vol. 39, pp. 1779–1783, Oct. 1991.
[20] M.-H. Murgulescu, E. Moisan, P. Legaud, E. Penard, and I. Zaquine, "New wideband, $.67\lambda_g$ circumference 180° hybrid ring coupler," *Electron. Lett.*, vol. 30, no. 4, pp. 299–300, Feb. 1994.

Brad Ryan Heimer was born in San Antonio, TX, on August 28, 1972. He received the B.S.E.E. and M.S.E.E. degrees from Texas A&M University, College Station, in 1995 and 1997, respectively.

During the summers of 1991 to 1995, he worked in the Electromagnetics and Microwave Laboratory, Texas A&M University, and at Texas Instruments, Dallas, TX. He is currently with Raytheon TI Systems, Dallas, TX, where his interests include MMIC and module design.

Lu Fan (M'96) received the B.S. degree in electrical engineering from Nanjing Institute of Technology (now Southeast University), Nanjing, China, in 1982.

From September 1982 to December 1990, he was with the Department of Radio Engineering, Nanjing Institute of Technology, as a Teaching Assistant and Lecturer. In 1991, he became a Research Associate in the Department of Electrical Engineering, Texas A&M University, College Station, TX. His research interests include microwave and millimeter-wave components and active antennas.

Kai Chang (S'75–M'76–SM'85–F'91) received the B.S.E.E. degree from the National Taiwan University, Taipei, Taiwan, R.O.C., the M.S. degree from the State University of New York at Stony Brook, and the Ph.D. degree from the University of Michigan at Ann Arbor, in 1970, 1972, and 1976, respectively.

From 1972 to 1976, he worked for the Microwave Solid-State Circuits Group, Cooley Electronics Laboratory, University of Michigan at Ann Arbor, as a Research Assistant. From 1976 to 1978, he was employed by Shared Applications, Inc., Ann Arbor, MI, where he worked in computer simulation of microwave circuits and microwave tubes. From 1978 to 1981, he worked for the Electron Dynamics Division, Hughes Aircraft Company, Torrance, CA, where he was involved in the research and development of millimeter-wave solid-state devices and circuits, power combiners, oscillators and transmitters. From 1981 to 1985, he worked for TRW Electronics and Defense, Redondo Beach, CA, as a Section Head, developing state-of-the-art millimeter-wave integrated circuits and subsystems including mixers, VCO's, transmitters, amplifiers, modulators, upconverters, switches, multipliers, receivers, and transceivers. In August 1995, he joined the Electrical Engineering Department, Texas A&M University, College Station, as an Associate Professor, and in 1988, became a Professor. In January 1990, he was appointed E-Systems Endowed Professor of electrical engineering. His current interests are in microwave and millimeter-wave devices and circuits, microwave integrated circuits, integrated antennas, wideband and active antennas, phased arrays, microwave power transmission, and microwave optical interactions. He has authored or coauthored *Microwave Solid-State Circuits and Applications* (Wiley, 1994), *Microwave Ring Circuits and Antennas* (Wiley, 1996), and *Integrated Active Antennas and Spatial Power Combining* (Wiley, 1996). He served as the editor of the four-volume *Handbook of Microwave and Optical Components* (Wiley, 1989, 1990), and is the editor of the Microwave and Optical Technology Letters and the Wiley Book Series in Microwave and Optical Engineering. He has also published over 250 technical papers and several book chapters in the areas of microwave and millimeter-wave devices, circuits, and antennas.

Dr. Chang received the Special Achievement Award from TRW in 1984, the Halliburton Professor Award in 1988, the Distinguished Teaching Award in 1989, the Distinguished Research Award in 1992, and the TEES Fellow Award in 1996 from Texas A&M University.